Video Article

Expansion of Two-dimension Electrospun Nanofiber Mats into Three-dimension Scaffolds

Emily Keit[1], Shixuan Chen[1], Hongjun Wang[1], Jingwei Xie[1]

[1]Department of Surgery-Transplant and Mary & Dick Holland Regenerative Medicine Program, University of Nebraska Medical Center

Correspondence to: Jingwei Xie at jingwei.xie@unmc.edu

URL: https://www.jove.com/video/58918
DOI: doi:10.3791/58918

Keywords: Electrospun nanofibers, subcritical CO_2, expand, two-dimension mats, three-dimension scaffolds, drug delivery, antimicrobial peptides, tissue regeneration

Date Published: 12/14/2018

Citation: Keit, E., Chen, S., Wang, H., Xie, J. Expansion of Two-dimension Electrospun Nanofiber Mats into Three-dimension Scaffolds. *J. Vis. Exp.* (), e58918, doi:10.3791/58918 (2018).

Abstract

Electrospinning has been the preferred technology in producing a synthetic, functional scaffold due to the biomimicry to extracellular matrix and the ease control of composition, structure, and diameter of fibers. However, despite these advantages, traditional electrospun nanofiber scaffolds come with limitations including disorganized nanofiber orientation, low porosity, small pore size, and mainly two-dimensional mats. As such, there is a great need for developing a new process for fabricating electrospun nanofiber scaffolds that can overcome the above limitations. Herein, a novel and simple method is outlined. A traditional 2D nanofiber mat is transformed into a 3D scaffold with desired thickness, gap distance, porosity, and nanotopographic cues to allow for cell seeding and proliferation through the depressurization of subcritical CO_2 fluid. In addition to providing a scaffold for tissue regeneration to occur, this method also provides the opportunity to encapsulate bioactive molecules such as antimicrobial peptides for local drug delivery. The CO_2 expanded nanofiber scaffolds hold great potential in tissue regeneration, wound healing, 3D tissue modeling, and topical drug delivery.

Video Link

The video component of this article can be found at https://www.jove.com/video/58918/

Introduction

The concept of developing a synthetic scaffold that can be implanted into patients to aid in tissue repair and regeneration is one that has permeated the regenerative medicine field for decades. The ideal synthetic scaffold serves to induce cell migration from surrounding healthy tissue, provides an architecture for cell seeding, adhesion, signaling, proliferation, and differentiation, supports vascularization, allows for adequate oxygenation and nutrition delivery, and promotes host immune activity to ensure success after implantation[1]. Additionally, it can be used as a carrier for embedding antimicrobial molecules to assist in wound healing[1,3,6,7,8,9]. The ability to control the temporal release of these biologic molecules from the synthetic scaffold is another desirable attribute that is considered when engineering scaffolds[1].

Electrospinning has been a well-utilized technique for producing nanofiber scaffolds[1,2,3,4,5,6]. Previous attempts to create a nanofiber scaffold such as the one discussed here have been done to varying degrees of success. However, traditional nanofiber scaffolds have limited abilities to achieve these goals. Traditional nanofiber scaffolds have been mostly two-dimensional mats[1,3]. These nonexpanded scaffolds are densely packed with small pore sizes; this limits cell infiltration, migration, and differentiation as it does not promote an environment similar enough to those found *in vivo*[1,7,8,9]. For this reason, newer techniques of 3D electrospun nanofiber scaffold preparation have been established to amend the inherent flaws that come with 2D nanofiber mats. These techniques result in 3D scaffolds; however, they have limited applicability due to the production methods requiring aqueous solutions and freeze-drying procedures. This processing results in the random distribution of the nanofibers without restricted organization, proper thickness, and/or desired porosity to provide the adequate nanotopographic cues that are necessary for cell migration and proliferation. These factors result in the previous 3D electrospun nanofiber scaffolds that lack adequate mimicry of living tissues[1,7,8,9].

More recent attempts at developing an expanded, 3D scaffold with better biomimicry of extracellular matrix (ECM) have been performed using an aqueous sodium borohydride ($NaBH_4$) solution treatment and predesigned molds to aid in better control of the shape of the resulting scaffold[7,8]. However, this method is not ideal as it requires the use of aqueous solutions, chemical reactions, and freeze-drying that may interfere with polymers and any encapsulated biomolecules that are water-soluble. The additives used may also cause side effects during tissue regeneration[8,9]. The CO_2 expansion method outlined in this article greatly reduces processing time, eliminates the need for aqueous solutions, and preserves the amount and functionality of biologically active molecules to a greater extent than the previously established methods[9].

In previous studies, antibiotics, silver, 1α,25 dihydroxyvitamin D_3, and antimicrobial peptide LL-37 were loaded into the nanofiber scaffolds individually and in combination to investigate the potential of these scaffolds to release agents to further aid in wound healing[9,10,12,13]. For the purpose of demonstrating this method of nanofiber scaffold expansion, Coumarine 6, a fluorescent dye, will be loaded into the scaffold to demonstrate the potential of embedding the scaffold with various desired compounds. This method of expanded nanofiber scaffold fabrication in

conjunction with encapsulated bioactive molecules holds great potential in tissue regeneration, wound healing, the creation of 3D tissue models, and the topical delivery of drugs.

Protocol

All *in vivo* procedures outlined below were approved by the IACUC Committee at the University of Nebraska Medical Center.

1. Prepare the Solutions for Standard Electrospinning

1. In a 20 mL glass tube, dissolve 2 g of poly(ε-caprolactone) (PCL, Mw= 80 kDa) in a solvent mixture of dichloromethane (DCM) and N,N-dimethylformamide (DMF) with a 4:1 ration (v/v) at a concentration of 10% (w/v).
   CAUTION: Handle DCM and DMF in a well-ventilated hood to avoid exposure to fumes. Do not expose DCM to plastic materials.
2. Place the glass tube into a lab rotator until the solution becomes clear. The solution may mix overnight.
3. If intending to embed bioactive materials such as peptides or drugs into the scaffold, create a separate solution and store at the 4 °C until ready to use.
   1. Prepare the fluorescent dye solution (50 mg/mL) using 20 mL of PCL solution.

2. Set Up the Electrospinning Apparatus (Figure 1A)

1. Add the PCL solution to a 20 mL syringe with a 21 gauge blunt needle attached. Ensure that there is no air in the syringe and associated tubing.
2. Place a rotating steel drum with the ground collector 12 cm from the needle tip.
3. Using alligator clips, connect the Direct Current (DC) High Voltage power supply to the needle and ensure that the collector is grounded.
   CAUTION: Always turn off the power supply before handling any connected materials.

3. Electrospinning

1. For the 20 mL of PCL solution, set the parameters of the syringe pump as follows: diameter = 20.27 mm, flow rate = 0.5 mL/h. Check if the droplets are forming at the tip of the needle.
2. If the incorporation of bioactive molecules is desired, set up the apparatus to allow for co-axial electrospinning **(Figure 1B)**. Create a customized coaxial nozzle using hypodermic needles.
   NOTE: Such nozzles are also available commercially. Note that a solution of dye is prepared to simulate the adding such molecules.
   1. Prepare a 1% solution of the fluorescent dye Coumarin 6 in water. Add 3 mL of the 1% dye to a small syringe. Connect the syringe to the same coaxial nozzle as the PCL solution. Once again, ensure that there are no air bubbles.
   2. For this 3 mL solution, set the parameters of the syringe pump as follows: diameter = 9.49 mm, flow rate = 0.02 mL/h. Check if the droplets are forming at the tip of the needle.
3. Apply an electric potential of 20 kV between the spinneret (22-gauge needle) and a ground collector located 20 cm away from the spinneret. Collect the aligned nanofiber mats in a drum rotating at 2000 rpm. Collect the PCL nanofiber mats once they reach a thickness of ~1 mm.

4. Generation of PCL Nanofiber Mats with Arrayed Holes.

1. Fabricate PCL nanofiber mats.
   1. Dissolve PCL beads in a solvent mixture consisting of DCM and DMF with a ratio of 4:1(v/v) at a concentration of 10% (PCL) (w/v). Pump the PCL solution at a flow rate of 0.7 mL/h using a syringe pump while a potential of 20 kV is applied between the spinneret (a 22-gage needle) and a grounded collector located 12 cm apart from the spinneret.
   2. Collect the nanofiber membrane using a rotating drum with a rotating speed larger than 500 rpm.
2. Immerse the PCL nanofiber mats in liquid N_2 for 5 min (*i.e.*, become stiff). Keep the PCL nanofiber mats in liquid N_2 and punch PCL nanofiber mats with a 0.5 mm-diameter punch.

5. Expansion of 2D Nanofiber Mats with/without Arrayed Holes *via* Subcritical CO_2 Liquid (Figure 2).

1. Place the PCL nanofiber mats into liquid nitrogen for 5 min and cut into 1 cm x 1 cm squares using sharp surgical scissors while submerged in liquid nitrogen to avoid deformation of the edges.
2. Place the cut mat in a 30 mL centrifuge tube with ~1 g of dry ice. Tightly cap the lid and allow for the dry ice to change into liquid CO_2.
3. Once liquid has formed in the tube, quickly release the pressure by opening the cap.
   CAUTION: Use proper thermal protective gear when working with liquid nitrogen and dry ice. Do not open the pressurized tube towards the face. The centrifuge tube should not be used repeatedly.
4. Remove and observe the puffed scaffold from the tube. Place the scaffold in a new centrifuge tube with dry ice and repeat until the desired thickness is achieved. Sterilize the expanded nanofiber scaffolds in ethylene oxide prior to incubation with cells.

6. Characterization of Expanded Nanofiber Scaffolds

1. Characterize the morphology and structure of the expanded nanofiber scaffolds using scanning electron microscopy (SEM).
    1. Place the samples with double-sided conductive tape to the metallic stud and coat with platinum for 40 s using a sputter coater at 40 mA.
    2. Examine the fibers using SEM according to previous studies[9]. Collect the images at an accelerating voltage of 15 kV.

2. Characterize *in vitro* release profiles and bioactivity of released peptides.
    1. Weight 10 mg of nanofiber membranes before and after the expansion in CO_2.
    2. Immerse the samples in PBS buffer and collect 10 µL of supernatant at different time points (0-28 days).
    3. Use Enzyme-Linked Immuno Sorbent Assay (ELISA) kit to quantify the LL-37 peptide concentration in the collected supernatant.

3. Examine cellular infiltration *in vivo* and host response.
    1. Put the 9-week old Sprague-Dawley (SD) rats in an anesthesia chamber, connect to isoflurane vapor and anesthetize the rats. Transfer the rats to an operating table after the rats become complete anesthesia without feelings. Continuously anesthetize the rats using an isoflurane-nose cone with vaporizer during the surgery. Shave the hair of rat's backs by an animal's shaver and sterilize it with iodine and alcohol skin scrub. Create subcutaneous pockets via 1.5 cm incisions at supraspinal sites on the dorsum using a scalpel.
    2. Insert one expanded nanofiber scaffold (1.5 mm-thick) into the subcutaneous pocket using tweezers for each incision. Close the incision using a stapler.
    3. At 1, 2, and 4 weeks, euthanize the rats with 95% CO_2. Gently dissect the explant and the surrounding tissue using surgical scissors. Prior to histological analysis, immerse the tissue in formalin for at least 3 days, and then embed with paraffin. Section the tissue with a microtome, then perform hematoxylin and eosin (H&E), Masson's trichrome staining.

Representative Results

The efficacy of expanding traditional 2D electrospun nanofiber mats into 3D scaffolds via depressurization of subcritical CO_2 fluid was demonstrated in different capacities: the thickness of the scaffolds increased from 1 mm when untreated to 2.5 mm and 19.2 mm with one and two CO_2 treatments, respectively (**Figure 3A-C**). The porosity-a characteristic of the architecture critical for cell seeding-also increased in a manner corresponding to the increased thickness (**Figure 3C**). The porosity of the scaffolds increased from 79.5% for the untreated mats to 92.1 and 99.0% after the first and second treatments, respectively (**Figure 3D**). This is significant because the degree of cell penetration into a scaffold and thus its efficacy to induce regeneration is largely dependent on the porosity[1].

SEM images revealed that the densely packed, fibrillar structure of untreated 2D mats were transformed into ordered, layered structures with aligned nanofibers after expansion with CO_2 (**Figure 3E-H**). Previous studies have concluded that similarly layered structures with organized fibers could be critical in the preservation of nanotopographic cues for the regeneration of tissues such as tendon, muscle, and nerve[7,8]. However, these studies examined the scaffolds expanded with $NaBH_4$[7,8]. This method requires extra processing time and solvents that may leach bioactive molecules from the scaffold[7,8]. $NaBH_4$, a strong reducing agent, could react with encapsulated bioactive molecules. Conversely, the use of subcritical CO2 fluid for expansion was shown to preserve the bioactivity of the additional molecules pre-seeded into the scaffold when compared with scaffolds expanded using the $NaBH_4$ method (**Figure 4**). This was demonstrated using Coumarin 6 dye; the green color of the dye was better retained in the scaffolds expanded with CO_2 (**Figure 4**), indicating that the use of subcritical CO_2 fluid for expansion results in better retention of the integrity of molecules encapsulated in the PCL scaffolds.

The release kinetics of the antimicrobial peptide LL-37 from the scaffolds before and after expansion were measured *in vitrovia* an ELISA kit according to manufacturer's instructions (**Figure 5A**). The antimicrobial efficacy of LL-37 peptide-loaded nanofiber scaffolds before and after expansion with CO_2 was evaluated *via* the incubation with *Pseudomonas aeruginosa* (*P. aeruginosa*). The number of living colonies post incubation with the scaffolds was quantified. The results showed that the antimicrobial activity of the CO_2-expanded, LL-37-loaded scaffolds was similar to that of unexpanded LL-37-loaded scaffolds, indicating that the expanding process can preserve the bioactivity of encapsulated LL-37 peptides (**Figure 5B**).

Further *in vivo* studies were carried out by subcutaneous implantation of CO_2-expanded nanofiber scaffolds with square-arrayed holes to rats. This allows for cellular migration and proliferation within the holes as well as further infiltration within the nanofiber layers that were created during expansion (**Figure 6**). The expanded scaffold showed a significant increase in the number of blood vessels formed (**Figure 6C, E**) and multinucleated giant cells (**Figure 6D, F**) from week 1 to 4 post implantation. Further immunohistological staining results indicated a decrease of the number of C-C chemokine receptor type 7 (CCR7)-positive infiltrated macrophages and an increase of the number of Cluster of Differentiation 206(CD206)-positive infiltrated macrophages from week 1 to week 4 after implantation.

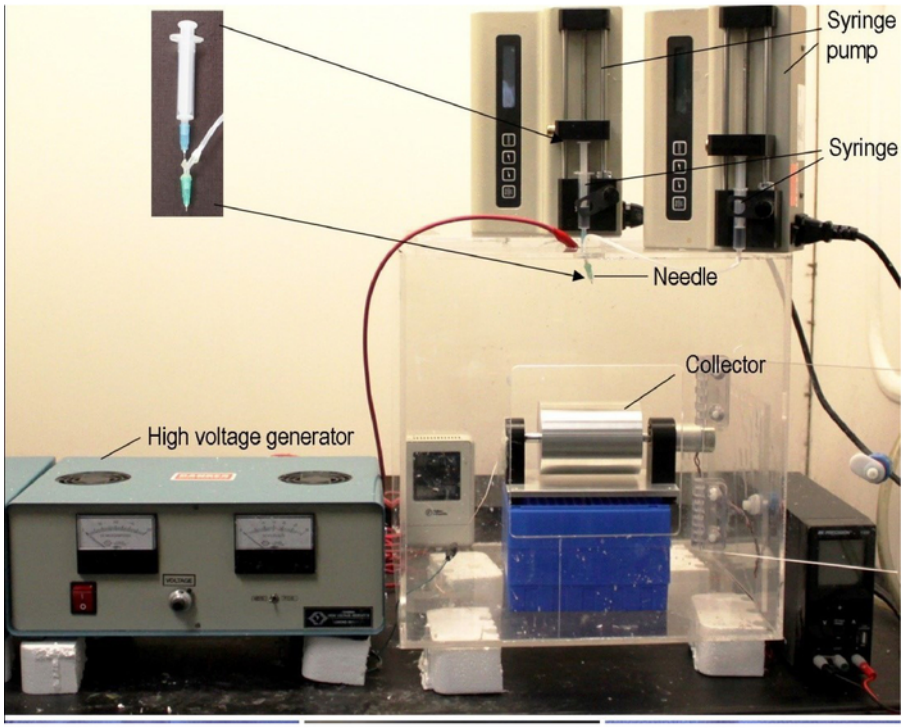

Figure 1: Typical electrospinning setup. A typical coaxial electrospinning apparatus is shown. Electrospinning requires three major components: a high-voltage power supply, a spinneret, and an electrically conductive collector. Coaxial spinning uses two liquids to spin a nanofiber scaffold; this allows for the encapsulation of other molecules. Nanofiber alignment and assemblies can be augmented through the collector by varying the rotational speeds of the rotating drum. In this protocol, a customized nozzle was created using two hypodermic needles. Similar nozzles are available commercially. This figure has been adapted from Xie, *et al*[14]. Please click here to view a larger version of this figure.

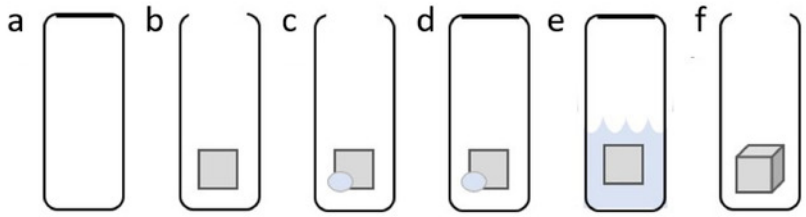

Figure 2: Steps of scaffold expansion using subcritical CO_2 fluid. (A) Use a container that is sealable and can withstand pressure, such as a 30 mL plastic centrifuge tube. **(B)** Add a 1 cm x 1 cm piece of 2D PCL nanofiber mat. **(C)** Add ~1 g of dry ice. **(D)** Seal the container. **(E)** Allow pressure to build in the tube. This will turn the solid CO_2 into liquid CO_2. When liquid has gathered, quickly release the seal of the tube. This will cause the liquid CO_2 to quickly become gaseous CO_2, resulting in CO_2 permeating the 2D nanofiber mat. **(F)** Observe the 3D scaffold. These steps may be repeated until the desired thickness is achieved. Please click here to view a larger version of this figure.

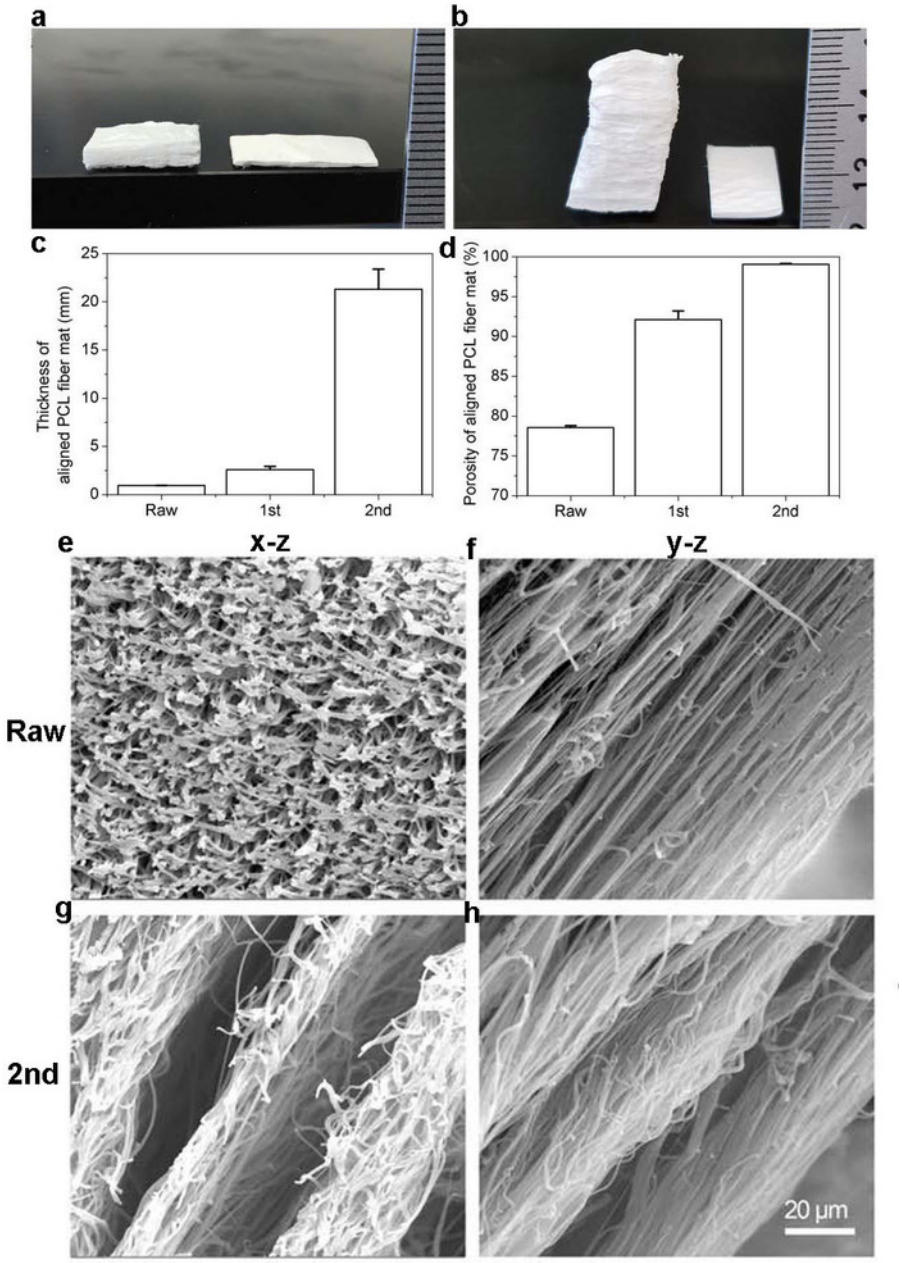

Figure 3: Visualization of 2D mats before and after expansion with CO_2 subcritical fluid. (A) Photograph shows PCL nanofiber mats before the treatment of subcritical CO_2 fluid (right) and after the first treatment (left). **(B)** Photograph shows PCL nanofiber mat before the first treatment with CO_2 subcritical fluid (right) and after the second treatment (left). **(C)** Graph shows the thicknesses of PCL fiber mats before and after one and two treatments with subcritical CO_2 fluid. **(D)** Graph shows the relative porosity of PCL fiber mats before and after one and two treatments with subcritical CO_2 fluid. **(E-H)** Image shows cross-sectional appearance of PCL mats captured via SEM. **(E-F)** SEM image of PCL fiber mats before treatment. **(G-H)** SEM image of PCL fiber mats after two treatments with subcritical CO_2 fluid. This figure has been adapted from Jiang, *et al*[9]. Please click here to view a larger version of this figure.

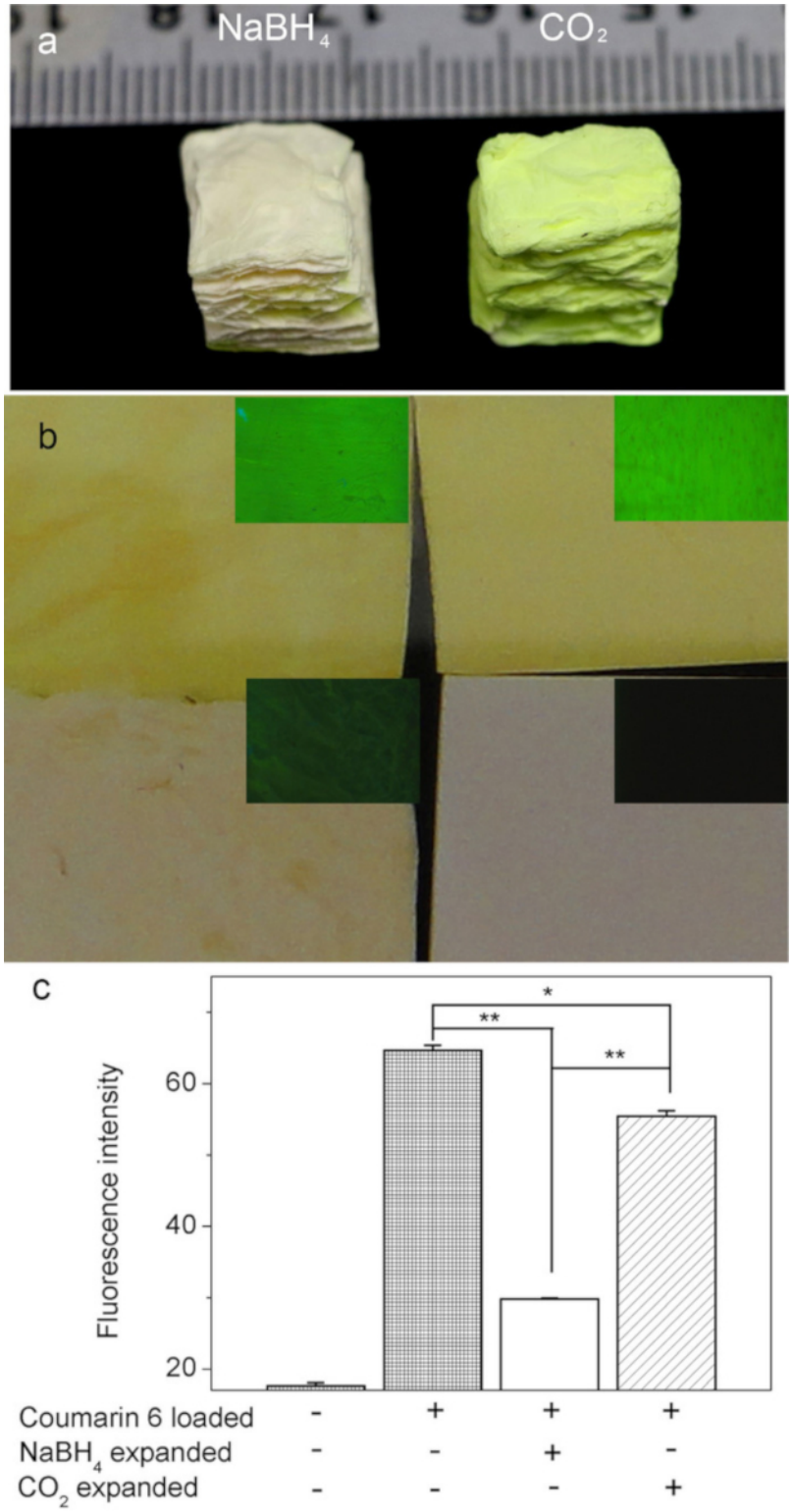

Figure 4: Coumarin 6 dye-loaded PCL nanofiber mats before and after expansion with subcritical CO_2 fluid and $NaBH_4$ aqueous solution. (A) Images grossly show the amount of Coumarine 6 dye remaining in PCL scaffolds following expansion with CO_2 (right) and $NaBH_4$ (left). **(B)** Images show gross top views of PCL scaffolds and their corresponding fluorescence in the following order: Raw scaffold (bottom right), 2D mat loaded with Coumarine 6 dye (top right), PCL scaffold loaded with Coumarine 6 dye expanded with CO_2 (top left), $NaBH_4$ (bottom left). **(C)** Graph shows the fluorescence intensity of Coumarin 6 dye after PCL mats were untreated, expanded via subcritical CO_2 fluid, and expanded via $NaBH_4$ treatments. Fluorescence was quantified by Image J software. This figure has been adapted from Jiang, *et al*[9]. Please click here to view a larger version of this figure.

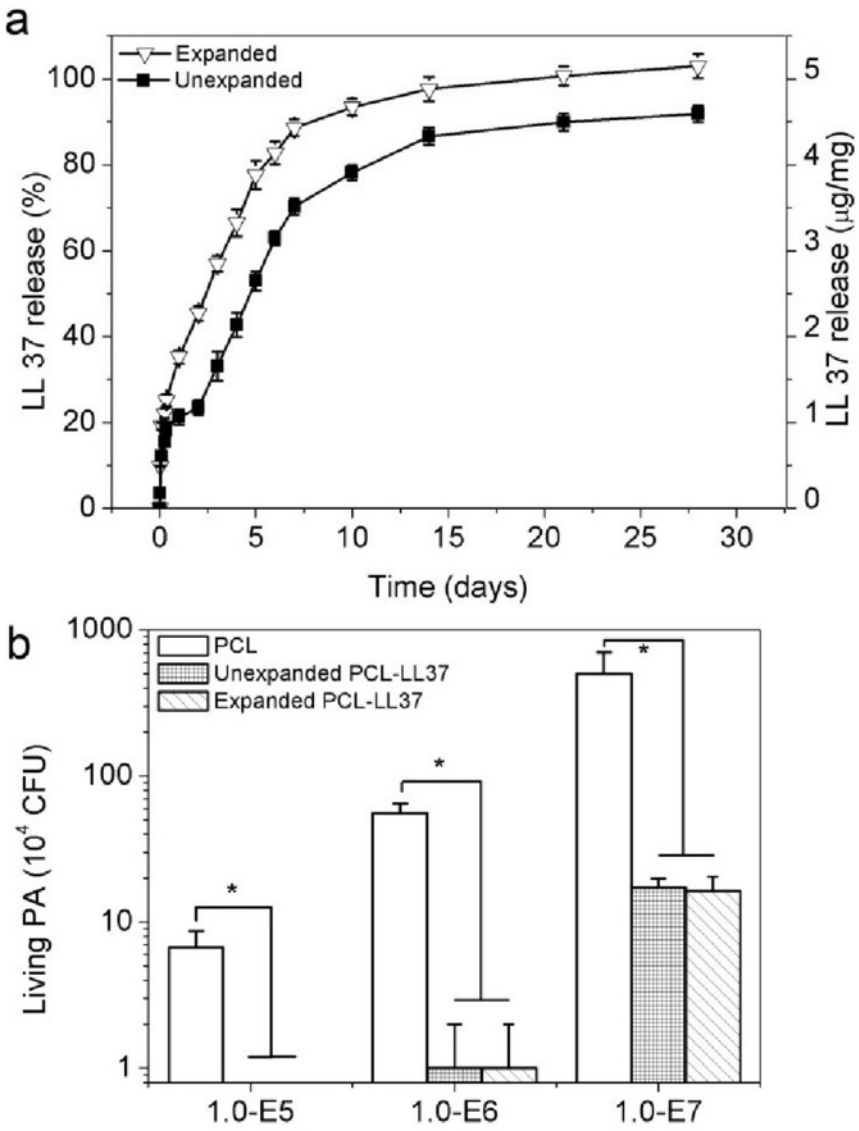

Figure 5: Bioactive molecules encapsulated in PCL scaffolds. **(A)** Graph depicts the relative release of antimicrobial peptide LL-37 in 2D membranes and subcritical CO_2 fluid expanded 3D scaffolds **(B)** Graphs depict the antimicrobial efficacy of different PCL nanofiber mats when exposed to *P. aeruginosa*. This figure has been adapted from Jiang, *et al*[9]. Please click here to view a larger version of this figure.

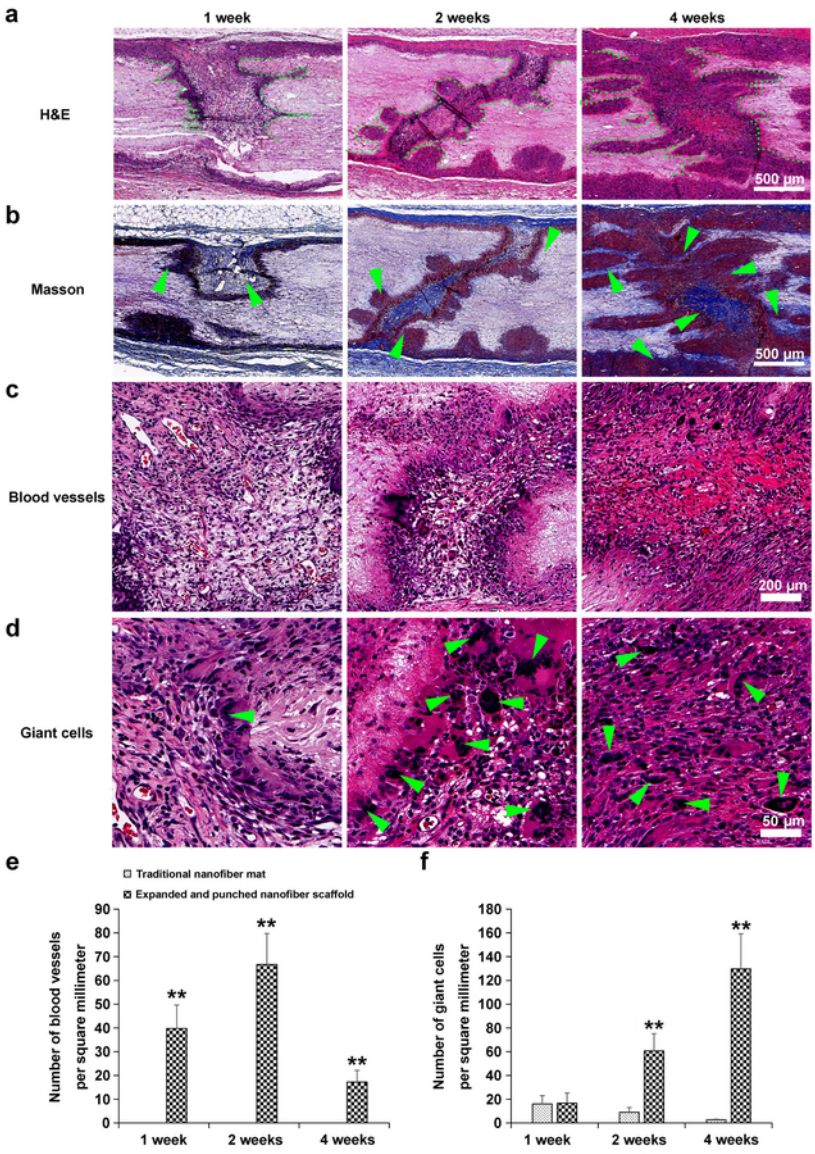

Figure 6: *In vivo* responses of PCL nanofiber scaffolds with and without expansion *via* subcritical CO_2 in subcutaneous dorsum sites of rats. (A) H&E stain. Green dots designate boundaries of cell infiltration. **(B)** Masson's trichrome stain. Green arrows designate collagen deposition. **(C)** Highly magnified image of H&E stain. Green arrows designate blood vessels. **(D)** Highly magnified images of H&E stain. Green arrows designate giant cells. **(E)** Graph depicts the growth of blood vessels per mm^2. **(F)** Graph quantifies the number of giant cells that infiltrate into traditional 2D PCL mats compared with PCL mats expanded with subcritical CO_2. This figure has been adapted from Jiang, *et al*[9]. Please click here to view a larger version of this figure.

Discussion

Transforming traditional 2D electrospun nanofiber mats into expanded 3D scaffolds *via* CO_2 depressurization was investigated. Traditional 2D nanofiber mats are successfully expanded *via* subcritical CO_2 fluid. The critical steps are to fabricate 2D nanofiber mats under an optimized condition and cut the mats without deforming the edges (*e.g.*, using sharp surgical scissors). This CO_2-expanded nanofiber scaffolds have many benefits over traditional 2D mats including layered structures (**Figure 3A-B**), less packing density (**Figure 3D-H**), and higher porosity (**Figure 3D**). This expansion method is also advantageous relative to the existing methods of expansion in that it is quicker to process and reduces the overall loss of encapsulated active biologic molecules due to this technique's exclusion of aqueous solutions and freeze-drying procedures[8,9]. However, the limitation of this technique is that the morphology of polymeric nanofibers should not be deformed/dissolved in the subcritical CO_2 fluid. For example, PLGA (50:50) nanofiber mats cannot be expanded using this technique. Such nanofiber mats could be expanded using other gas liquids.

Our previous studies demonstrated that cells seeded in a more uniform manner within expanded nanofiber scaffolds when compared with 2D mats[8]. In this work, a significantly increased rate of blood vessel formation occurred (**Figure 6C, E**), and host immune cell infiltrates were observed within CO_2-expanded nanofiber scaffolds with square-arrayed holes following subcutaneous implantation in rats (**Figure 6D, F**).

Angiogenesis and immune cell infiltration indicate that the scaffold is engaging with the host tissue and possibly homing cells necessary for regeneration of the damaged tissue; this implies a higher rate of success post-implantation into the host[9].

The CO_2-expanded scaffolds also have the potential to be incorporated with a variety of peptides and other molecules that can aid in obtaining the desired response. Here, the desired effect is to be a scaffold for tissue regeneration while simultaneously providing antimicrobial activity through the incorporated LL-37 peptide. The scaffolds expanded with subcritical CO_2 fluid also showed better retention of the incorporated molecules when compared with scaffolds expanded with $NaBH_4$. The dye molecules encapsulated within the PCL scaffolds were better retained (**Figure 4**). Additionally, a slightly greater proportion of the antimicrobial peptide LL-37 encapsulated was released from the 3D CO_2 expanded scaffolds when compared to 2D mats (**Figure 5A**). The bioactivity of LL-37 was retained as the CO_2 expanded scaffolds showed a similar antimicrobial efficacy when compared to the 2D scaffolds (**Figure 5B**).

This new method of 3D expansion that signifies the synthetic scaffold production is no longer limited to the use of 2D nanofiber mats. The data presented suggests that this expansion method better maintain the amount and bioactivity of encapsulated bioactive materials within expanded nanofiber scaffolds. Simultaneously, the expanded nanofiber scaffolds mimic the nanotopographic environments of those found *in vivo*[9], an attribute that greatly assists in inducing tissue regeneration[1]. In the future, these CO_2-expanded scaffolds may have potential applications in the assistance of wound healing and tissue regeneration as well as in 3D tissue model creation and locally controlled drug delivery.

Disclosures

Authors declare that there is no conflict of interest.

Acknowledgements

This work was supported by grants from the National Institute of General Medical Science (NIGMS) at the NIH (2P20 GM103480-06 and 1R01GM123081 to J.X.), the Otis Glebe Medical Research Foundation, NE LB606, and startup funds from the University of Nebraska Medical Center.

References

1. Chen, S., *et al.* Recent advances in electrospun nanofibers for wound healing. *Nanomedicine.* **12** (11), 1335-1352 (2017).
2. Khandalavala, K., Jiang, J., Shuler, F. D., Xie, J. Electrospun Nanofiber Scaffolds with Gradations in Fiber Organization. *Journal of Visualized Experiments.* (98), e52626 (2015).
3. Xie, J., Li, X., Xia, Y. Put electrospun nanofibers to work for biomedical research. *Macromolecular Rapid Communication.* **29** (22), 1775-1792 (2008).
4. Xie, J., *et al.* Nanofiber membranes with controllable microwells and structural cues and their use in forming cell microarrays and neuronal networks. *Small.* **7** (3), 293-297 (2011).
5. Xie, J., *et al.* Radially aligned, electrospun nanofibers as dural substitutes for wound closure and tissue regeneration applications. *ACS nano.* **4** (9), 5027-5036 (2010).
6. Xie, J., *et al.* "Aligned-to-random" nanofiber scaffolds for mimicking the structure of the tendon-to-bone insertion site. *Nanoscale.* **2** (6), 923-926 (2010).
7. Jiang, J., *et al.* Expanded 3D Nanofiber Scaffolds: Cell Penetration, Neovascularization, and Host Response. *Advanced Healthcare Materials.* **5** (23), 2993-3003 (2016).
8. Jiang, J., *et al.* Expanding Two-Dimensional Electrospun Nanofiber Membranes in the Third Dimension by a Modified Gas-Foaming Technique. *ACS Biomaterials Science & Engineering.* **10** (1), 991-1001 (2015).
9. Jiang, J., *et al.* CO2-expanded nanofiber scaffolds maintain activity of encapsulated bioactive materials and promote cellular infiltration and positive host response. *Acta Biomaterialia.* **68**, 237-248 (2018).
10. Chen, S., *et al.* Nanofiber-based sutures induce endogenous antimicrobial peptide. *Nanomedicine.* **12** (10), 2597-2609 (2017).
11. Dhand, C., *et al.* Bio-inspired crosslinking and matrix-drug interactions for advanced wound dressings with long-term antimicrobial activity. *Biomaterials.* **138**, 153-168 (2017).
12. Jiang, J. *et al.* Local sustained delivery of 25-hydroxyvitamin D3 for production of antimicrobial peptides. *Pharmaceutical Research.* **32** (9), 2851-2862 (2015).
13. Jiang, J. *et al.* 1α, 25-dihydroxyvitamin D_3-eluting nanofibrous dressings induce endogenous antimicrobial peptide expression. *Nanomedicine (Lond).* **13** (12), 1417-1432 (2018).
14. Ma, B., Xie, J., Jiang, J., Shuler, F.D., Bartlett, D.E. Rational design of nanofiber scaffolds for orthopedic tissue repair and regeneration. *Nanomedicine.* **8** (9), 1459-1481 (2013).

